Network Architecture and Mutational Sensitivity of the *C. elegans* Metabolome

Lindsay M. Johnson[1*], Luke M. Chandler[2*], Sarah K. Davies[3] and Charles F. Baer[1,2]

1 – Department of Biology, University of Florida, Gainesville, FL

2 – University of Florida Genetics Institute

3 - Faculty of Medicine, Department of Surgery & Cancer, Imperial College, London

* - these authors contributed equally

Email: lindsaymjohnson@ufl.edu; lukemchandler@ufl.edu; sarah.davies1@imperial.ed.uk

Correspondence to:

Charles F. Baer

Department of Biology

University of Florida

P. O. Box 118525

Gainesville, FL 32611-8525 USA

Email: cbaer@ufl.edu

Keywords: metabolic network, mutation accumulation, mutational correlation, mutational variance, network centrality

Declarations:

- Ethics approval and consent to participate: Not applicable
- Consent for publication: Not applicable
- Availability of data and material:
  - Metabolomics data (normalized metabolite concentrations) are archived in Dryad (http://dx.doi.org/10.5061/dryad.2dn09/1).
  - Data used to reconstruct the metabolic networks are included in Supplementary Appendix A1.
- Competing interests: The authors declare no competing interests.
- Funding: Funding was provided by NIH grant R01GM107227 to CFB and E. C. Andersen. The funding agency had no role in the design of the study and the collection, analysis, and interpretation of the data or in the writing of the manuscript.
- Authors' contributions. LMJ and LMC collected and analyzed data in the network reconstruction and contributed to writing the manuscript. SKD collected and analyzed the GC-MS data. CFB analyzed data and wrote the manuscript. All authors read and approved the final manuscript.
- Acknowledgements: This work was initially conceived by Armand Leroi and Jake Bundy. We thank Art Edison, Dan Hahn, Tom Hladish and especially Hongwu Ma for their generosity and very helpful advice.

List of Figures and Tables

Abstract

Background: A fundamental issue in evolutionary systems biology is understanding the relationship between the topological architecture of a biological network, such as a metabolic network, and the evolution of the network. The rate at which an element in a metabolic network accumulates genetic variation via new mutations depends on both the size of the mutational target it presents and its robustness to mutational perturbation. Quantifying the relationship between topological properties of network elements and the mutability of those elements will facilitate understanding the variation in and evolution of networks at the level of populations and higher taxa.

Results: We report an investigation into the relationship between two topological properties of 29 metabolites in the *C. elegans* metabolic network and the sensitivity of those metabolites to the cumulative effects of spontaneous mutation. The relationship between several measures of network centrality and sensitivity to mutation is weak, but point estimates of the correlation between network centrality and mutational variance are positive, with only one exception. There is a marginally significant correlation between core number and mutational heritability. There is a small but significant negative correlation between the shortest path length between a pair of metabolites and the mutational correlation between those metabolites.

Conclusions: Positive association between the centrality of a metabolite and its mutational heritability is consistent with centrally-positioned metabolites presenting a larger mutational target than peripheral ones, and is inconsistent with centrality conferring mutational robustness, at least *in toto*. The weakness of the correlation between shortest path length and the mutational correlation between pairs of metabolites suggests that network locality is an important but not overwhelming factor governing mutational pleiotropy. These findings provide

88 necessary background against which the effects of other evolutionary forces, most importantly
89 natural selection, can be interpreted.
90

Introduction:

The set of chemical reactions that constitute organismal metabolism is often represented as a network of interacting components, in which individual metabolites are the nodes in the network and the chemical reactions of metabolism are the edges linking the nodes [1]. Representation of a complex biological process such as metabolism as a network is conceptually powerful because it offers a convenient and familiar way of visualizing the system, as well as a well-developed mathematical framework for analysis.

If the representation of a biological system as a network is to be useful as more than a metaphor, it must have predictive power [2]. Metabolic networks have been investigated in the context of evolution, toward a variety of ends. Many studies have compared empirical metabolic networks to various random networks, with the goal of inferring adaptive features of network architecture (e.g., [1, 3-7]. Other studies have addressed the relationship between network-level properties of individual elements of the network (e.g., node degree, centrality) and properties such as rates of protein evolution [8, 9] and within-species polymorphism [10].

One fundamental evolutionary process that remains essentially unexplored with respect to metabolic networks is mutation. Mutation is the ultimate source of genetic variation, and as such provides the raw material for evolution: the greater the input of genetic variation by mutation, the greater the capacity for evolution. However, in a well-adapted population, most mutations are at least slightly deleterious. At equilibrium, the standing genetic variation in a population represents a balance between the input of new mutations that increase genetic variation and reduce fitness, and natural selection, which removes deleterious variants and thereby increases fitness. Because genetic variation is jointly governed by mutation and selection, understanding the evolution of any biological entity, such as a metabolic network, requires an independent accounting of the effects of mutation and selection.

The cumulative effects of spontaneous mutations can be assessed in the near absence of natural selection by means of a mutation accumulation (MA) experiment (Figure 1). Selection

117 becomes ineffective relative to random genetic drift in small populations, and mutations with
118 effects on fitness smaller than about the reciprocal of the population size (technically, the
119 genetic effective population size, N_e) will be essentially invisible to natural selection [11]. An MA
120 experiment minimizes the efficacy of selection by minimizing N_e, thereby allowing all but the
121 most strongly deleterious mutations to evolve as if they are invisible to selection [12].
122 Our primary interest is in the relationship between the centrality of a metabolite in the
123 network and the sensitivity of that metabolite to mutation. Roughly speaking, the centrality of a
124 node in a network quantifies some measure of the importance of the node in the network [13].
125 A generic property of empirical networks, including metabolic networks, is that they are
126 (approximately) scale-free; scale-free networks are characterized by a topology with a few "hub"
127 nodes (high centrality) and many peripheral nodes (low centrality; [1]). Scale-free networks are
128 more robust to random perturbation than are randomly-connected networks [14].
129 Mutation is an important source of perturbation to biological systems, and much effort
130 has gone into theoretical and empirical characterization of the conditions under which
131 mutational robustness will evolve [15-17]. Mutational robustness can be assessed in two basic
132 ways: top-down, in which a known element of the system is mutated and the downstream
133 effects of the mutation quantified, or bottom-up, in which mutations are introduced at random,
134 either spontaneously or by mutagenesis, and the downstream effects quantified. Top-down
135 experiments are straightforward to interpret: the greater the effects of the mutation (e.g., on a
136 phenotype of interest), the less robust the system. However, the scope of inference is limited to
137 the types of mutations introduced by the investigator (which in practice are almost always gene
138 knockouts), and provide limited insight into natural variation in mutational robustness.
139 Bottom-up approaches, in which mutations are allowed to accumulate at random,
140 provide insight into the evolution of a system as it actually exists in nature: all else equal, a
141 system, or element of a system ("trait"), that is robust to the effects of mutation will accumulate
142 less genetic variance under MA conditions than one that is not robust (Figure 1b; [18]).

However, the inference is not straightforward, because all else may not be equal: different systems or traits may present different mutational targets (roughly speaking, the number of sites in the genome that potentially affect a trait; [19]).

Ultimately, disentangling the evolutionary relationship between network architecture, mutational robustness, and mutational target is an empirical enterprise, specific to the system of interest. As a first step, it is necessary to establish the relationship between network architecture (e.g., topology) and the rate of accumulation of genetic variance under MA conditions. If a general relationship emerges, targeted top-down experiments can then be employed to dissect the relationship in more mechanistic detail.

In addition to the relationship between metabolite centrality and mutational variance, we are also interested in the relationship between network topology and the mutational correlation (r_M) between pairs of metabolites (Figure 1c). In principle, mutational correlations reflect pleiotropic relationships between genes underlying pairs of traits (but see below for caveats; [20]). Genetic networks are often modular [21], consisting of groups of genes (modules) within which pleiotropy is strong and between which pleiotropy is weak [22]. Genetic modularity implies that mutational correlations will be negatively correlated with the length of the shortest path between network elements. However, it is possible that the network of gene interactions underlying metabolic regulation is not tightly correlated with the metabolic network itself, e.g., if *trans* acting regulation predominates.

Here we report results from a long-term MA experiment in the nematode *Caenorhabditis elegans*, in which replicate MA lines derived from a genetically homogeneous common ancestor (G0) were allowed to evolve under minimally effective selection ($N_e \approx 1$) for approximately 250 generations (Figure 1a). We previously reported estimates from these MA lines of two key quantitative genetic parameters by which the cumulative effects of mutation can be quantified: the per-generation change in the trait mean (the mutational bias, ΔM) and the per-generation increase in genetic variation (the mutational variance, V_M) for the standing pools of 29

metabolites [23]; Supplementary Table S1. In this report, we interpret those results, and new estimates of mutational correlations (r_M), in the context of the topology of the *C. elegans* metabolic network.

Results and Discussion

Representation of the Metabolic Network – The metabolic network of *C. elegans* was estimated in two ways: *(i)* by the method of Ma and Zeng [24; MZ],and *(ii)* by the method of Yilmaz and Walhout [25; YW]. Details of the network construction are given in section I of the Methods; data are presented in Supplementary Appendix A1. For the set of metabolites included (see Methods), MZ and YW give nearly identical results. In the few cases in which there is a discrepancy (~1%; Supplementary Table S2), we use the MZ network, for reasons we explain in the Methods. The resulting network is a directed graph including 646 metabolites, with 1203 reactions connecting nearly all metabolites (Figure 2).

Properties of networks can be quantified in many ways, and different measures of centrality capture different features of network importance (Table 1). We did not have a strong prior hypothesis about which specific measure(s) of centrality would prove most informative in terms of a relationship with ΔM and/or V_M. Therefore, we assessed the relationship between mutational properties and several measures of network centrality: betweenness, closeness, and degree centrality, in- and out-degree, and core number (depicted in Figure 3). These parameters are all positively correlated. Definitions of the parameters are given in Table 1; correlations between the parameters are included in Table 2. For each of the six parameters, we calculated Spearman's correlation ρ between mutational statistics and the network parameter associated with the metabolite. The strict experiment-wide 5% significance level for these correlations is approximately $P<0.002$ (α=0.05/[6 network parameters x 4 mutational parameters]).

Mutational Parameters – Details of the MA experiment are reported in [26] and outlined in section II of the Methods. The experimental protocol by which metabolite concentrations were measured is reported in [23] and outlined in section III of the Methods; data are archived in Dryad at http://dx.doi.org/10.5061/dryad.2dn09/1. For each of the 29 metabolites, the cumulative effects of mutation are summarized by the mutational bias (ΔM), and the mutational variance (V_M). For a trait z, $\Delta M_z = \mu_G \alpha_z$, where μ_G is the genomic mutation rate and α_z is the average effect of a mutation on the trait; $V_M = \mu_G \alpha_z^2$ [27, p. 329]. Details of the estimation of mutational parameters are given in section IV of the Methods.

Comparisons of variation among traits or groups require that the variance be measured on a common scale. V_M is commonly scaled either relative to the trait mean, in which case V_M is the squared coefficient of variation and is often designated I_M, or relative to the residual variance, V_E; V_M/V_E is the mutational heritability, h_M^2. I_M and h_M^2 have different statistical properties and evolutionary interpretations [28], so we report both. I_M and I_E are standardized relative to the mean of the MA lines.

Network centrality and sensitivity to mutation –

(i) Mutational bias (ΔM). It is reasonable to expect that metabolite concentrations are under some degree of stabilizing selection, in which case sufficiently large changes in either direction are deleterious. Neither ΔM nor |ΔM| showed a clear association with any measure of network centrality (Table 1). Four metabolites (adenosine, nicotinamide, succinic acid, and xanthine) have atypically large, positive ΔM (Supplementary Table S1), among the largest values of ΔM ever reported for any trait [23], and those four metabolites all have core number $k = 2$ ($P = 0.03$, exact probability). However, the large ΔM for those traits is probably an artifact of scaling, because those four metabolites had very low concentrations (near zero) in the G0 ancestor.

(ii) Mutational variance (V_M). We report V_M scaled in two ways: relative to the trait mean (I_M) and relative to the residual ("environmental") variance, h_M^2. Of the twelve correlations (two measures of mutational variance × six measures of centrality), the correlation with betweenness centrality

is very slightly negative; the rest are positive (Table 2), although only the correlation between core number and h_M^2 approaches statistical significance at the experiment-wide 5% level (ρ=0.48, P<0.008). The 29 metabolites in our data set have core number of either one or two (the maximum core number of any metabolite in the network is two). Mean h_M^2 of metabolites of core number = 2 is approximately 2.5X greater than that of metabolites of core number = 1 (0.002 vs. 0.0008). To put that result in context, the average h_M^2 for a wide variety of traits in a wide variety of organisms is on the order of 0.001 [28].

Core number is a discrete interval variable, whereas the other measures of network centrality are continuous variables. As an alternative analysis, we performed ordinary linear regression (equivalent to analysis of variance in the case of a binary categorical variable) of $\log(h_M^2)$ on core number; the results are similar to the rank correlation ($F_{1,27} = 10.53$, P<0.0032; Pearson's $r = 0.53$).

The conservative interpretation of these results is that there is no relationship between network centrality and any measure of mutational sensitivity. If so, there are various possible explanations. For example, it may be that mutational target and mutational robustness effectively cancel each other out. More worryingly, it may be that the representation of the *C. elegans* metabolic network used here misrepresents the network as it actually exists *in vivo*. The topology of the dynamic metabolic network of the bacterium *E. coli* varies depending on the environmental context [29], and it seems intuitive that the greater spatiotemporal complexity inherent to a multicellular organism would exacerbate that problem. More mundanely, it may be that the sampling variance associated with the relatively small number of mutations and MA lines drowns out any signal of an association. Or it may be that there simply is no functional relationship between the centrality of a metabolite in a network and its sensitivity to mutation.

The liberal interpretation is that the near-significant correlation of mutational heritability with core number represents a weak signal emerging from a small sample from a noisy system.

Quantifying centrality in terms of core number is analogous to categorizing a set of size measurements into "small" and "large": power is increased, at the cost of losing the ability to discriminate between more subtle differences.

The raw mutational variance, V_M, appears in the numerator of both h_M^2 and I_M; the difference lies in the denominator, which is the residual variance V_E for h_M^2 and the square of the trait mean for I_M. For some replicates of some metabolites, estimated metabolite concentrations were atypically low and near zero; I_M is more sensitive to low outliers than is h_M^2. However, the correlation between I_M and the trait mean is small (r = -0.11) and not significantly different from zero. Alternatively, it is possible that V_M does not vary consistently with metabolite centrality, but that metabolites with low centrality (core number = 1) are more susceptible to random microenvironmental variation ("noise") than are metabolites with high centrality (core number = 2), in which case V_E would be greater for metabolites with low centrality and h_M^2 would be lower. Unfortunately, the variance is correlated with the trait mean, so the least biased way to address that question is by comparing the residual squared coefficients of variation, I_E. There is no hint of correlation between core number and I_E (ρ=0.025, P>0.89; Table 2), and I_E is uncorrelated with the trait mean (r = -0.12, P>0.54), so the association between h_M^2 and core number cannot obviously be attributed to differential sensitivity to random noise.

The relationship between mutational correlation (r_M) and shortest path length – In an MA experiment, the cumulative effects of mutations on a pair of traits *i* and *j* may covary for two, nonexclusive reasons [20]. More interestingly, individual mutations may have consistently pleiotropic effects, such that mutations that affect trait *i* also affect trait *j* in a consistent way. Less interestingly, but unavoidably, individual MA lines will have accumulated different numbers of mutations, and if mutations have consistently directional effects, as would be expected for traits correlated with fitness, lines with more mutations will have more extreme trait values than lines with fewer mutations, even in the absence of consistent pleiotropy. Estes et al. [20]

simulated the sampling process in *C. elegans* MA lines with mutational properties derived from empirical estimates from a variety of traits and concluded that sampling is not likely to lead to large absolute mutational correlations in the absence of consistent pleiotropy ($|r_M| \leq 0.25$).

Ideally, we would like to estimate the full mutational (co)variance matrix, ***M,*** from the joint estimate of the among-line (co)variance matrix. However, with 25 traits, there are (25x26)/2 = 325 covariances, and with only 43 MA lines, there is insufficient information to jointly estimate the restricted maximum likelihood of the full ***M*** matrix. To proceed, we calculated mutational correlations from pairwise REML estimates of the among-line (co)variances, i.e., $r_M = \frac{COV_L(X,Y)}{\sqrt{VAR_L(X)VAR_L(Y)}}$ [30, 31]. Pairwise estimates of r_M are shown in Supplementary Table S3. To assess the extent to which the pairwise correlations are sensitive to the underlying covariance structure, we devised a heuristic bootstrap analysis. For a random subset of 12 of the 300 pairs of traits, we randomly sampled six of the remaining 23 traits without replacement and estimated r_M between the two focal traits from the joint REML among-line (co)variance matrix. For each of the 12 pairs of focal traits, we repeated the analysis 100 times.

There is a technical caveat to the preceding bootstrap analysis. Resampling statistics are predicated on the assumption that the variables are exchangeable [32], which metabolites are not. For that reason, we do not present confidence intervals on the resampled correlations, only the distributions. However, we believe that the analysis provides a meaningful heuristic by which the sensitivity of the pairwise correlations to the underlying covariance structure can be assessed.

Distributions of resampled correlations are shown in Supplementary Figure S2. In every case the point estimate of r_M falls on the mode of the distribution of resampled correlations, and in 11 of the 12 cases, the median of the resampled distribution is very close to the point estimate of r_M. However, in six of the 12 cases, some fraction of the resampled distribution falls outside two standard errors of the point estimate. The most important point that the resampling

295 analysis reveals is this: given that 29 metabolites encompass only a small fraction of the total
296 metabolome of *C. elegans* (<5%), even had we been able to estimate the joint likelihood of the
297 full 29x30/2 ***M***-matrix, the true covariance relationships among those 29 metabolites could
298 conceivably be quite different from those estimated from the data.

299 Correlations are properties of pairs of variables, so we expect *a priori* that network
300 parameters that apply to pairs of elements are more likely to contain information about the
301 mutational correlation between a pair of metabolites than will the pairwise average of a
302 parameter that applies to individual elements of a network. The shortest path length is the
303 simplest network property that describes the relationship between two nodes, although since the
304 metabolic network is directed, the shortest path from element *i* to element *j* is not necessarily
305 the same as the shortest path from *j* to *i*. For each pair of metabolites *i* and *j*, we calculated the
306 shortest path length from *i* to *j* and from *j* to *i*, without repeated walks (Supplementary Table S4).
307 We then calculated Spearman's correlation ρ between the mutational correlation r_M and the
308 shortest path length.

309 Statistical assessment of the correlation between mutational correlations (r_M) and
310 shortest path length presents a problem of nonindependence, for two reasons. First, all
311 correlations including the same variable are non-independent. Second, even though the
312 mutational correlation between metabolites *i* and *j* is the same as the correlation between *j* and
313 *i*, the shortest path lengths need not be the same, and moreover, the path from *i* to *j* may exist
314 whereas the path from *j* to *i* may not. To account for non-independence of the data, we devised
315 a parametric bootstrap procedure; details are given in section V of the Methods. Three
316 metabolites (L-tryptophan, L-lysine, and Pantothenate) lie outside of the great strong component
317 of the network [33] and are omitted from the analysis.

318 There is a weak, but significant, negative correlation between r_M and the shortest path
319 length between the two metabolites (ρ = -0.128, two-tailed P<0.03; Supplementary Figure S1a),
320 whereas $|r_M|$ is not significantly correlated with shortest path length (ρ = -0.0058, two-tailed

P>0.45; Supplementary Figure S1b). The correlation between r_M and the shortest path in the undirected network is similar to the correlation between r_M and the shortest path in the directed network (ρ = -0.105, two-tailed P>0.10; Supplementary Figure S1c).

An intuitive possible cause of the weak negative association between shortest path length and mutational correlation would be if a mutation that perturbs a metabolic pathway toward the beginning of the pathway has effects that propagate downstream in the same pathway, but the effect of the perturbation attenuates. The attenuation could be due either to random noise or to the effects of other inputs into the pathway downstream from the perturbation (or both). The net effect would be a characteristic pathway length past which the mutational effects on two metabolites are uncorrelated, leading to an overall negative correlation between r_M and path length. The finding that the correlations between r_M and the shortest path length in the directed and undirected network are very similar reinforces that conclusion. The negative correlation between r_M and shortest path length is reminiscent of a finding from Arabidopsis, in which sets of metabolites significantly altered by single random gene knockouts are closer in the global metabolic network than expected by chance [34].

Conclusions and Future Directions

The proximate goal of this study was to find out if there are topological properties of the *C. elegans* metabolic network (node centrality, shortest path length) that are correlated with a set of statistical descriptions of the cumulative effects of spontaneous mutations (ΔM, V_M, r_M). Ultimately, we hope that a deeper understanding of those mathematical relationships will shed light on the mechanistic biology of the organism. Bearing in mind the statistical fragility of the results, we conclude:

(i) Network centrality may be associated with mutational sensitivity (V_M), it is not associated with mutational robustness ($1/V_M$). If the liberal interpretation of the results is true, the most plausible explanation is that metabolites that are central in the network present a larger mutational target than do metabolites that peripherally located. However, although $1/V_M$ is a meaningful measure

of mutational robustness [35], it does not necessarily follow that highly-connected metabolites are therefore more robust to the effects of *individual* mutations [19, 36].

(ii) Pleiotropic effects of mutations affecting the metabolome are predominantly local, as evidenced by the significant negative correlation between shortest path length between a pair of metabolites and the mutational correlation, r_M, between that pair of metabolites. That result is not surprising in hindsight, but the weakness of the correlation suggests that there are other important factors that underlie pleiotropy beyond network proximity.

To advance understanding of the mutability of the *C. elegans* metabolic network, three things are needed. First, it will be important to cover a larger fraction of the metabolic network. Untargeted mass spectrometry of cultures of *C. elegans* reveals many thousands of features (Art Edison, personal communication); 29 metabolites are only the tip of a large iceberg. For example, our intuition leads us to believe that the mutability of a metabolite will depend more on its in-degree (mathematically, the number of edges leading into a node in a directed graph; biochemically, the number of reactions in which the metabolite is a product) than its out-degree. The point-estimate of the correlation of h_M^2 with in-degree is twice that of the correlation of h_M^2 with out-degree (Table 2), although the difference is not statistically significant.

Second, to more precisely partition mutational (co)variance into within- and among-line components, more MA lines are needed. We estimate that each MA line carries about 80 unique mutations (see Methods), thus the mutational (co)variance is the result of about 3500 total mutations, distributed among 43 MA lines. The MA lines were a preexisting resource, and the sample size was predetermined. It is encouraging that we were able to detect significant mutational variance for 25/29 metabolites (Supplementary Table S1b), but only 14% (42/300) of pairwise mutational correlations are significantly different from zero at the experiment-wide 5% significance level, roughly corresponding to $|r_M|>0.5$ (Supplementary Table S3); 18 of the 42 significant mutational correlations are not significantly different from $|r_M| = 1$. It remains uncertain how sensitive estimates of mutational correlations are to the underlying covariance

373 structure of the metabolome. It also remains to be seen if the mutability of specific features of
374 metabolic networks are genotype or species-specific, and the extent to which mutability
375 depends on environmental context.

376 Third, it will be important to quantify metabolites (static concentrations and fluxes) with
377 more precision. The metabolite data analyzed in this study were collected from large cultures
378 (n>10,000 individuals) of approximately age-synchronized worms, and were normalized relative
379 to an external quantitation standard [23]. Ideally, one would like to characterize the
380 metabolomes of single individuals, assayed at the identical stage of development. That is not
381 yet practical with *C. elegans*, although it is possible to quantify hundreds of metabolites from a
382 sample of 1000 individuals [37], and preliminary studies suggest it will soon be possible to
383 reduce the number of individuals to 100 or even ten (M. Witting, personal communication).
384 Minimizing the number of individuals in a sample is important for two reasons; (1) the smaller
385 the sample, the easier it is to be certain the individuals are closely synchronized with respect to
386 developmental stage, and (2) knowing the exact number of individuals in a sample makes
387 normalization relative to an external standard more interpretable. Ideally, data would be
388 normalized relative to both an external standard and an internal standard (e.g., total protein;
389 [30]).

390 This study provides an initial assessment of the relationship between mutation and
391 metabolic network architecture. To begin to uncover the relationship between metabolic
392 architecture and natural selection, the next step is to repeat these analyses with respect to the
393 standing genetic variation (VG). There is some reason to think that more centrally-positioned
394 metabolites will be more evolutionarily constrained (i.e., under stronger purifying selection) than
395 peripheral metabolites [8], in which case the ratio of the mutational variance to the standing
396 genetic variance (VM/VG) will increase with increasing centrality.

397

398 **Methods and Materials:**

399 I. Metabolic Network:

400 The metabolic network of *C. elegans* was estimated in two ways: *(i)* by the static, purely
401 graphical method of Ma and Zeng ([24]; updated at http://www.ibiodesign.net/kneva/; we refer to
402 this method as MZ), and *(ii)* by the dynamical, flux-balance analysis (FBA) method of Yilmaz
403 and Walhout ([25]; http://wormflux.umassmed.edu/; we refer to this method as YW).
404 Subnetworks that do not contain at least one of the 29 metabolites were excluded from
405 downstream analyses. The MZ method includes several *ad hoc* criteria for retaining or omitting
406 specific metabolites from the analysis (criteria are listed on p. 272 of [24]). The set of reactions
407 in the MZ and YW networks are approximately 99% congruent; in the few cases in which there
408 is a discrepancy (listed in Supplementary Table S2), we chose to use the MZ network because
409 we used the MZ criteria for categorizing currency metabolites (defined below).

410 To begin, the 29 metabolites of interest were identified and used as starting sites for the
411 network. Next, all forward and reverse reactions stemming from the 29 metabolites were
412 incorporated into the subnetwork until all reactions either looped back to the starting point or
413 reached an endpoint. Currency metabolites were removed following the MZ criteria (a currency
414 metabolite is roughly defined as a molecule such as water, proton, ATP, NADH, etc., that
415 appears in a large fraction of metabolic reactions but is not itself an intermediate in an
416 enzymatic pathway). Metabolic networks in which currency metabolites are included have much
417 shorter paths than networks in which they are excluded. When currency metabolites are
418 included in the network reported here, all shortest paths are reduced to no more than three
419 steps, and most shortest paths consist of one or two steps. The biological relevance of path
420 length when currency metabolites are included in the network is unclear [24].

421 A graphical representation of the network was constructed with the Pajek software
422 package (http://mrvar.fdv.uni-lj.si/pajek/) and imported into the networkX Python package [38],
423 which was used to generate network statistics. Proper importation from Pajek to networkX was
424 verified by visual inspection.

II. Mutation Accumulation Lines

A full description of the construction and propagation of the mutation accumulation (MA) lines is given in [26]. Briefly, 100 replicate MA lines were initiated from a nearly-isogenic population of N2-strain *C. elegans* and propagated by single-hermaphrodite descent at four-day (one generation) intervals for approximately 250 generations. The long-term N_e of the MA lines is very close to one, which means that mutations with a selective effect less than about 25% are effectively neutral [39]. The common ancestor of the MA lines ("G0") was cryopreserved at the outset of the experiment; MA lines were cryopreserved upon completion of the MA phase of the experiment. Based on extensive whole-genome sequencing [40; A. Saxena and CFB, in prep], we estimate that each MA line carries about 80 mutant alleles in the homozygous state.

At the time the metabolomics experiments reported in [23] were initiated, approximately 70 of the 100 MA lines remained extant, of which 43 ultimately provided sufficient material for Gas Chromatography/Mass Spectrometry (GC-MS). Each MA line was initially replicated five-fold, although not all replicates provided data of sufficient quality to include in subsequent analyses; the mean number of replicates included per MA line is 3.9 (range = 2 to 5). The G0 ancestor was replicated nine times. However, the G0 ancestor was not subdivided into "pseudolines" [41], which means that inferences about mutational variances and covariances are necessarily predicated on the assumption that the among-line (co)variance of the ancestor is zero. Each replicate consisted of age-synchronized young-adult stage worms taken from a single 10 cm agar plate.

III. Metabolomics:

Details of the extraction and quantification of metabolites are given in [23]. Briefly, samples were analyzed using an Agilent 5975c quadrupole mass spectrometer with a 7890 gas chromatograph. Metabolites were identified by comparison of GC-MS features to the Fiehn Library [42] using the AMDIS deconvolution software [43], followed by reintegration of peaks using the GAVIN Matlab script [44]. Metabolites were quantified and normalized relative to an

external quantitation standard. 34 metabolites were identified, of which 29 were ultimately included in the analyses. Normalized metabolite data are archived in Dryad (http://dx.doi.org/10.5061/dryad.2dn09).

IV. Quantitative Genetic Analyses: There are three quantitative genetic parameters of interest: *(i)* the per-generation proportional change in the trait mean, referred to as the mutational bias, ΔM; *(ii)* the per-generation increase in the genetic variance, referred to as the mutational variance, V_M; and *(iii)* the genetic correlation between the cumulative effects of mutations affecting pairs of traits, the mutational correlation, r_M. Details of the calculations of ΔM and V_M are reported in [23]; we reprise the basic calculations here.

(i) Mutational bias (ΔM) – The mutational bias is the change in the trait mean due to the cumulative effects of all mutations accrued over one generation. $\Delta M_z = \mu_G \alpha_z$, where μ_G is the per-genome mutation rate and α_z is the average effect of a mutation on trait *z*, and is calculated as $\Delta M_z = \frac{\bar{z}_{MA} - \bar{z}_0}{t\,\bar{z}_0}$, where $\bar{z}_{MA}$ and $\bar{z}_0$ represent the MA and ancestral (G0) trait means and *t* is the number of generations of MA.

(ii) Mutational variance (V_M) - The mutational variance is the increase in the genetic variance due to the cumulative effects of all mutations accrued over one generation. $V_M = \mu_G \alpha_z^2$ and is calculated as $V_M = \Delta V_L = \frac{V_{L,MA} - V_{L,G0}}{2t}$, where $V_{L,MA}$ is the variance among MA lines, $V_{L,G0}$ is the among-line variance in the G0 ancestor, and *t* is the number of generations of MA [27, p. 330]. In this study, we must assume that $V_{L,G0} = 0$.

(iii) Mutational correlation, r_M – Pairwise mutational correlations were calculated from the among-line components of (co)variance, which were estimated by REML as implemented in the in the MIXED procedure of SAS v. 9.4, following JD Fry [45]. Statistical significance of individual correlations was assessed by Z-test, with a global 5% significance criterion of approximately P<0.000167.

V. Analysis of the correlation between mutational correlation (r_M) and shortest path length - Each off-diagonal element of the 24x24 mutational correlation matrix (r_{ij}=r_{ji}) was associated with a random shortest path length sampled with probability equal to its frequency in the empirical distribution of shortest path lengths between all metabolites included in the analysis. Next, we calculated the Spearman's correlation ρ between r_M and the shortest path length. The procedure was repeated 10,000 times to generate an empirical distribution of ρ, to which the observed ρ can be compared. This comparison was done for the raw mutational correlation, r_M, the absolute value, $|r_M|$, and between r_M and the shortest path length in the undirected network (i.e., the shorter of the two paths between metabolites *i* and *j*).

Acknowledgments –

This work was initially conceived by Armand Leroi and Jake Bundy. We thank Art Edison, Dan Hahn, Tom Hladish, Marta Wayne, and especially Hongwu Ma for their generosity and very helpful advice. We thank the anonymous reviewers for their helpful comments. Support was provided by NIH grant R01GM107227 to CFB and E. C. Andersen.

References Cited

1. Jeong H, Tombor B, Albert R, Oltvai ZN, Barabasi AL: **The large-scale organization of metabolic networks**. *Nature* 2000, **407**(6804):651-654.

2. Winterbach W, Van Mieghem P, Reinders M, Wang HJ, de Ridder D: **Topology of molecular interaction networks**. *Bmc Systems Biology* 2013, **7**.

3. Minnhagen P, Bernhardsson S: **The Blind Watchmaker Network: Scale-Freeness and Evolution**. *PLoS One* 2008, **3**(2).

4. Wagner A, Fell DA: **The small world inside large metabolic networks**. *Proceedings of the Royal Society B-Biological Sciences* 2001, **268**(1478):1803-1810.

5. Fell DA, Wagner A: **The small world of metabolism**. *Nature Biotechnology* 2000, **18**(11):1121-1122.

6. Bernhardsson S, Minnhagen P: **Selective pressure on metabolic network structures as measured from the random blind-watchmaker network**. *New Journal of Physics* 2010, **12**.

7. Papp B, Teusink B, Notebaart RA: **A critical view of metabolic network adaptations**. *Hfsp Journal* 2009, **3**(1):24-35.

8. Vitkup D, Kharchenko P, Wagner A: **Influence of metabolic network structure and function on enzyme evolution**. *Genome Biology* 2006, **7**(5).

9. Greenberg AJ, Stockwell SR, Clark AG: **Evolutionary Constraint and Adaptation in the Metabolic Network of Drosophila**. *Molecular Biology and Evolution* 2008, **25**(12):2537-2546.

10. Hudson CM, Conant GC: **Expression level, cellular compartment and metabolic network position all influence the average selective constraint on mammalian enzymes**. *Bmc Evolutionary Biology* 2011, **11**.

11. Kimura M: **Evolutionary rate at the molecular level**. *Nature* 1968, **217**(5129):624-626.

514 12. Halligan DL, Keightley PD: **Spontaneous mutation accumulation studies in evolutionary**
515 **genetics**. *Annual Review of Ecology Evolution and Systematics* 2009, **40**:151-172.
516 13. Koschützki D, Schreiber F: **Centrality analysis methods for biological networks and their**
517 **application to gene regulatory networks**. *Gene Regulation and Systems Biology* 2008,
518 **2008**(2):193-201.
519 14. Albert R, Jeong H, Barabasi AL: **Error and attack tolerance of complex networks**. *Nature* 2000,
520 **406**(6794):378-382.
521 15. Wagner GP, Booth G, Bagheri HC: **A population genetic theory of canalization**. *Evolution* 1997,
522 **51**(2):329-347.
523 16. de Visser J, Hermisson J, Wagner GP, Meyers LA, Bagheri HC, Blanchard JL, Chao L, Cheverud JM,
524 Elena SF, Fontana W *et al*: **Perspective: Evolution and detection of genetic robustness**.
525 *Evolution* 2003, **57**(9):1959-1972.
526 17. Proulx SR, Nuzhdin SV, Promislow DEL: **Direct selection on genetic robustness revealed in the**
527 **yeast transcriptome**. *PLoS One* 2007, **2**(9):e911.
528 18. Stearns SC, Kaiser M, Kawecki TJ: **The differential genetic and environmental canalization of**
529 **fitness components in *Drosophila melanogaster***. *Journal of Evolutionary Biology* 1995,
530 **8**(5):539-557.
531 19. Houle D: **How should we explain variation in the genetic variance of traits?** *Genetica* 1998,
532 **103**:241-253.
533 20. Estes S, Ajie BC, Lynch M, Phillips PC: **Spontaneous mutational correlations for life-history,**
534 **morphological and behavioral characters in Caenorhabditis elegans**. *Genetics* 2005,
535 **170**(2):645-653.
536 21. Newman MEJ: **Modularity and community structure in networks**. *Proceedings of the National*
537 *Academy of Sciences of the United States of America* 2006, **103**(23):8577-8582.

538 22. Wagner GP, Pavlicev M, Cheverud JM: **The road to modularity**. *Nature Reviews Genetics* 2007,
539 **8**(12):921-931.
540 23. Davies SK, Leroi AM, Burt A, Bundy J, Baer CF: **The mutational structure of metabolism in**
541 ***Caenorhabditis elegans***. *Evolution* 2016.
542 24. Ma HW, Zeng AP: **Reconstruction of metabolic networks from genome data and analysis of**
543 **their global structure for various organisms**. *Bioinformatics* 2003, **19**(2):270-277.
544 25. Yilmaz LS, Walhout Albertha JM: **A *Caenorhabditis elegans* genome-scale metabolic network**
545 **model**. *Cell Systems* 2016, **2**(5):297-311.
546 26. Baer CF, Shaw F, Steding C, Baumgartner M, Hawkins A, Houppert A, Mason N, Reed M,
547 Simonelic K, Woodard W *et al*: **Comparative evolutionary genetics of spontaneous mutations**
548 **affecting fitness in rhabditid nematodes**. *Proceedings of the National Academy of Sciences of*
549 *the United States of America* 2005, **102**(16):5785-5790.
550 27. Lynch M, Walsh B: **Genetics and Analysis of Quantitative Traits**. Sunderland, MA.: Sinauer;
551 1998.
552 28. Houle D, Morikawa B, Lynch M: **Comparing mutational variabilities**. *Genetics* 1996,
553 **143**(3):1467-1483.
554 29. Koschützki D, Junker BH, Schwender J, Schreiber F: **Structural analysis of metabolic networks**
555 **based on flux centrality**. *Journal of Theoretical Biology* 2010, **265**(3):261-269.
556 30. Clark AG, Wang L, Hulleberg T: **Spontaneous mutation rate of modifiers of metabolism in**
557 **Drosophila**. *Genetics* 1995, **139**(2):767-779.
558 31. Mezey JG, Houle D: **The dimensionality of genetic variation for wing shape in *Drosophila***
559 ***melanogaster***. *Evolution* 2005, **59**(5):1027-1038.
560 32. Shaw RG: **Comparison of quantitative genetic parameters - reply**. *Evolution* 1992, **46**(6):1967-
561 1969.

562 33. Ma HW, Zeng AP: **The connectivity structure, giant strong component and centrality of**
563 **metabolic networks**. *Bioinformatics* 2003, **19**(11):1423-1430.
564 34. Kim T, Dreher K, Nilo-Poyanco R, Lee I, Fiehn O, Lange BM, Nikolau BJ, Sumner L, Welti R,
565 Wurtele ES *et al*: **Patterns of Metabolite Changes Identified from Large-Scale Gene**
566 **Perturbations in Arabidopsis Using a Genome-Scale Metabolic Network**. *Plant Physiology* 2015,
567 **167**(4):1685-U1890.
568 35. Stearns SC, Kawecki TJ: **Fitness sensitivity and the canalization of life-history traits**. *Evolution*
569 1994, **48**(5):1438-1450.
570 36. Ho WC, Zhang JZ: **Adaptive Genetic Robustness of Escherichia coli Metabolic Fluxes**. *Molecular*
571 *Biology and Evolution* 2016, **33**(5):1164-1176.
572 37. Witting M, Lucio M, Tziotis D, Wagele B, Suhre K, Voulhoux R, Garvis S, Schmitt-Kopplin P: **DI-**
573 **ICR-FT-MS-based high-throughput deep metabotyping: a case study of the Caenorhabditis**
574 **elegans-Pseudomonas aeruginosa infection model**. *Analytical and Bioanalytical Chemistry*
575 2015, **407**(4):1059-1073.
576 38. Hagberg AA, Schult DA, Swart PJ: **Exploring network structure, dynamics, and function using**
577 **NetworkX**. In: *7th Python in Science Conference (SciPy2008): 2008; Pasadena, CA USA*.
578 39. Keightley PD, Caballero A: **Genomic mutation rates for lifetime reproductive output and**
579 **lifespan in *Caenorhabditis elegans***. *Proceedings of the National Academy of Sciences of the*
580 *United States of America* 1997, **94**(8):3823-3827.
581 40. Denver DR, Wilhelm LJ, Howe DK, Gafner K, Dolan PC, Baer CF: **Variation in base-substitution**
582 **mutation in experimental and natural lineages of Caenorhabditis nematodes**. *Genome Biology*
583 *and Evolution* 2012, **4**(4):513-522.
584 41. Teotonio H, Estes S, Phillips PC, Baer CF: **Experimental Evolution with Caenorhabditis**
585 **Nematodes**. *Genetics* 2017, **206**(2):691-716.

586 42. Kind T, Wohlgemuth G, Lee do Y, Lu Y, Palazoglu M, S S, Fiehn O: **Mass spectral and retention**
587 **index libraries for metabolomics based on quadrupole and time-of-flight gas**
588 **chromatography/mass spectrometry.** *Analytical Chemistry* 2009 **81**:10038-10048.
589 43. Halket JM, Przyborowska A, Stein SE, Mallard WG, Down S, Chalmers RA: **Deconvolution gas**
590 **chromatography/mass spectrometry of urinary organic acids -- potential for pattern**
591 **recognition and automated identification of metabolic disorders**. *Rapid Communications in*
592 *Mass Spectrometry* 1999, **13**:279-284.
593 44. Behrends V, Tredwell GD, Bundy JG: **Gavin, a add-on to AMDIS, new GUI-driven version**.
594 *Analytical Biochemistry* 2011, **415** 206–208.
595 45. Fry JD: **Estimation of genetic variances and covariances by restricted maximum likelihood**
596 **using PROC MIXED**. In: *Genetic Analysis of Complex Traits Using SAS.* Edited by Saxton AM. Cary,
597 NC: SAS Institute, Inc.; 2004: 11-34.
598 46. Batagelj V, Zaversnik M: **Fast algorithms for determining (generalized) core groups in social**
599 **networks**. *Adv Data Anal Classif* 2011, **5**(2):129-145.
600
601

Figure Legends

Figure 1. (**a**) Schematic diagram of the mutation accumulation (MA) experiment. An MA experiment is simply a pedigree. The genetically homogeneous ancestral line (G0) was subdivided into 100 MA lines, of which 43 are included in this study. Lines were allowed to accumulate mutations for *t*=250 generations. At each generation, lines were propagated by a single randomly chosen hermaphrodite (N=1). Mutations, represented as colored blocks within a homologous pair of chromosomes, arise initially as heterozygotes and are either lost or fixed over the course of the experiment. At the culmination of the experiment, each line has accumulated its own unique set of mutations. MA lines were compared to the cryopreserved G0 ancestor, which is wild-type at all loci. After [12]. (**b**) Expected outcome of an MA experiment. As mutations accumulate over time, relative fitness (solid dark blue line) declines from its initial value of 1 at rate ΔM per generation and the genetic component of variance (solid orange line) increases from its initial value of 0 at rate V_M per generation. Trait X (light blue dashed line) is positively correlated with fitness and declines with MA; trait Y (green dashed line) is negatively correlated with fitness and increases with MA. Trajectories are depicted as linear, but they need not be. (**c**) Accumulation of mutational covariance in an MA experiment. Coordinate axes represent two traits, X and Y. Concentric ellipses show the increase in genetic covariance with MA, beginning from the initial value of zero; the orientation of the ellipses represents the linear relationship between pleiotropic mutational effects on the two traits.

Figure 2. Graphical depiction of the metabolic network including all 29 metabolites. Pink nodes represent included metabolites with core number = 1, red nodes represent included metabolites with core number = 2. Gray nodes represent metabolites with which the included 29 metabolites directly interact. Metabolite identification numbers are: 1, L-Serine; 2, Glycine; 3, Nicotinate; 4, Succinate; 5, Uracil; 6, Fumarate; 7, L-Methionine; 8, L-Alanine. 9, L-Aspartate;

10, L-3-Amino-isobutanoate; 11, trans-4-Hydroxy-L-proline; 12, (S) – Malate; 13, 5-Oxoproline; 14, L-Glutamate; 15, L-Phenylalanine; `6, L-Asparagine; 17, D-Ribose; 18, Putrescine; 19, Citrate; 20, Adenine; 21, L-Lysine; 22, L-Tyrosine; 23, Pantothenate; 24, Xanthine; 25, Hexadecanoic acid; 26, Urate; 27, L-Tryptophan; 28, Adenosine; 29, Alpha;alpha-Trehalose.

Figure 3. Schematic depiction of the *k*-cores of a graph. The *k*-core of a graph is the largest subgraph that contains nodes of degree at least *k*. The colored balls represent nodes in a network and the black lines represent connecting edges. Each red ball in the darkest gray area has core number *k*=3; note that each node with *k*=3 is connected to at least three other nodes. After Batagelj and Zaveršnik [46].

Figure 1

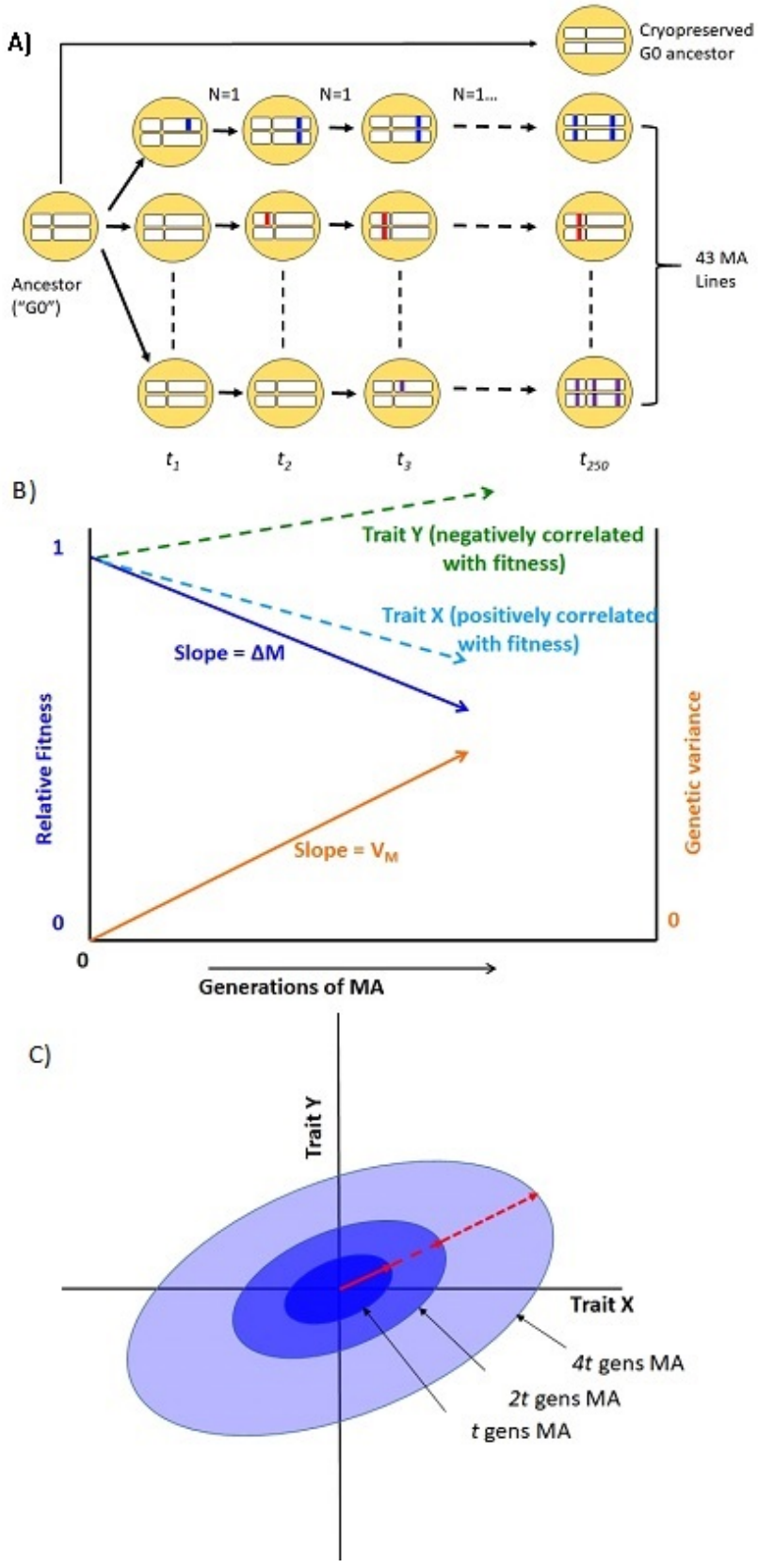

Figure 2

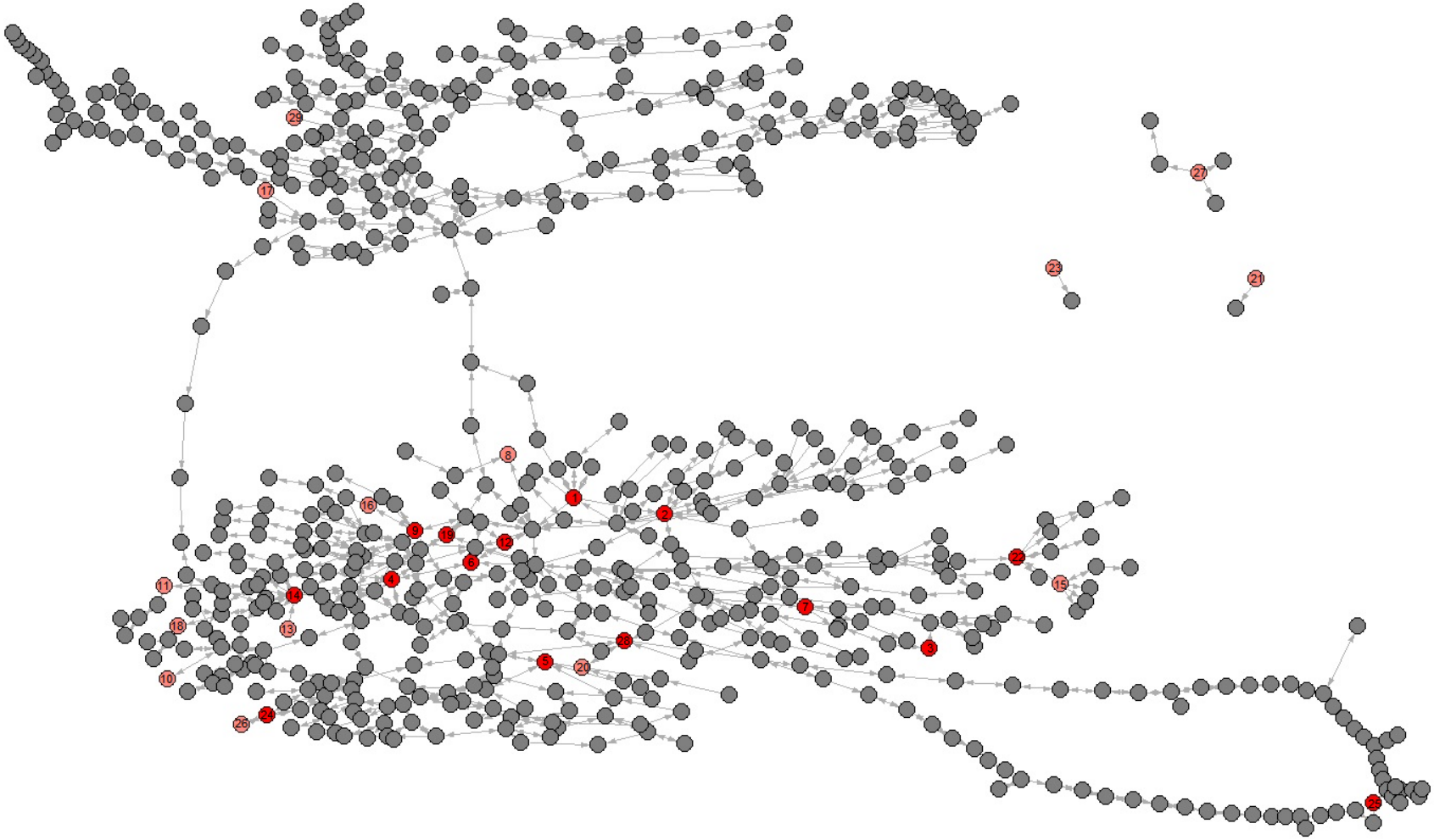

Figure 3

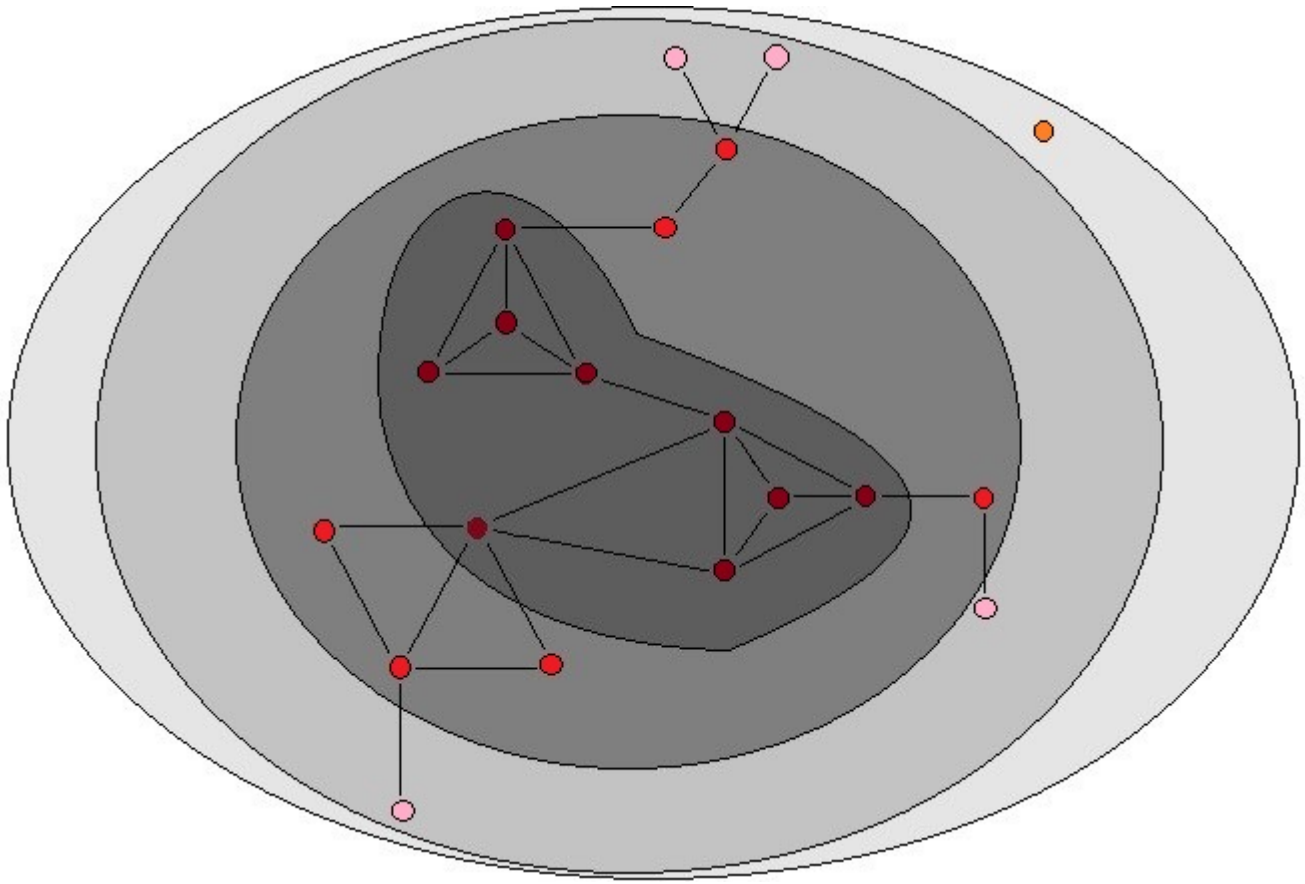

Parameter	Heuristic Definition	Formal Definition
In Degree (**IN°**), $deg^{+}(v)$	The number of incoming edges to node v in a directed graph.	self-explanatory
Out Degree (**OUT°**), $deg^{-}(v)$	The number of outgoing edges from node v in a directed graph.	self-explanatory
Shortest Path Length, $d(v,u)$	Shortest distance from node v to another node u with no repeated walks	self-explanatory
Betweenness Centrality (**BET**), $c_B(v)$	Betweenness centrality of node v is the sum of the fraction of all-pairs shortest paths that pass through v. The greater $c_B(v)$, the greater the fraction of shortest paths that pass through node v.	$\frac{c_B(v)}{(n-1)(n-2)}$, where $c_B(v) = \sum_{s,t \in V} \frac{\sigma(s,t\|v)}{\sigma(s,t)}$, *V* is the set of nodes, $\sigma(s,t)$ is the number of shortest paths from node *s* to node *t*, $\sigma(s,t\|v)$ is the number of paths from *s* to *t* that pass through node v, and *n* is the number of nodes in the graph. The denominator (*n*-1)(*n*-2) is the normalization factor for a directed graph that scales $c_B(v)$ between 0 and 1.
Closeness Centrality (**CLO**),	Closeness centrality of node v is the reciprocal of	$C(v) = \frac{n-1}{\sum_{u=1}^{n-1} d(u,v)}$, where *n* is the number of

Parameter	Heuristic Definition	Formal Definition
C(v)	the sum of the shortest path lengths to all *n*-1 other nodes, normalized by the sum of minimum possible distances *n-1*. The greater C(v), the closer v is to other nodes.	nodes and $d(u,v)$ is the shortest path distance between u and v.
Degree Centrality (**DEG**), $C_D(v)$	Degree centrality of node v is the fraction of nodes in the network that node v is connected to.	$C_D(v) = \frac{deg^+(v)+deg^-(v)}{n-1}$, where *n* is the number of nodes in the network.
Core Number (**CORE**)	A *k*-core is the largest subgraph that contains nodes of at least degree *k*. The core number of node v is the largest value *k* of a *k*-core containing node v.	Calculated using the algorithm of Batagelj and Zaversnik (2011).
Mutational Bias (**ΔM**)	Per-generation rate of change of the trait mean in an MA experiment. Equivalent to the product of the genome-wide mutation rate, μ_G, and the average effect of a mutation on the trait, α.	$\Delta M_z = \frac{\bar{z}_{MA}-\bar{z}_0}{t\bar{z}_0}$; $\bar{z}_{MA}$ and $\bar{z}_0$ represent the MA and ancestral (G0) trait means and *t* is the number of generations of MA.
Mutational Variance (V_M)	Per-generation rate of increase in genetic variance for a trait in an MA experiment.	$V_M = \Delta V_L = \frac{V_{L,MA}-V_{L,G0}}{2t}$, where $V_{L,MA}$ is the variance among MA lines, $V_{L,G0}$ is the among-

Parameter	Heuristic Definition	Formal Definition
	Equivalent to the product of the genome-wide mutation rate, μ_G, and the square of the average effect of a mutation on the trait, α^2.	line variance in the G0 ancestor, and *t* is the number of generations of MA
Squared coefficient of variation (I_M, I_E)	I_M is the mutational variance (V_M) scaled by the square of the trait mean, and provides a measure of the evolvability of a trait. I_E is the residual variance (V_E) scaled in the same way.	
Mutational heritability (h_M^2)	Mutational variance (V_M) scaled as a fraction of the residual variance (V_E). Provides a measure of the short-term response to selection on mutational variance.	$h_M^2 = \frac{V_M}{V_E}$
Mutational correlation (r_M)	Genetic correlation between two traits in MA lines. Provides an estimate of pleiotropic effects of new mutations.	$r_M = \frac{COV_M(X,Y)}{\sqrt{V_M(X)V_M(Y)}}$, where COV_M is the mutational covariance and V_M is the mutational variance.

Table 1. Definitions of network parameters, following the documentation of NetworkX, v.1.11 (Hagberg et al. 2008) and quantitative genetic parameters. Abbreviations of the parameters used in Table 2 follow the parameter name in parentheses in bold type.

	BTW	CLO	DEG	IN°	OUT°	CORE	ΔM	|ΔM|	I_M	I_E	h_M^2
BTW		0.60	0.84	0.86	0.66	0.79	-0.009 (0.96)	-0.055 (0.77)	-0.007 (0.97)	-0.122 (0.52)	0.128 (0.51)
CLO			0.54	0.51	0.47	0.54	0.012 (0.94)	0.297 (0.11)	0.119 (0.53)	0.034 (0.86)	0.089 (0.64)
DEG				0.88	0.92	0.83	0.038 (0.84)	-0.078 (0.68)	0.178 (0.35)	-0.062 (0.74)	0.218 (0.25)
IN°					0.65	0.85	0.099 (0.60)	0.043 (0.82)	0.188 (0.32)	0.007 (0.97)	0.277 (0.14)
OUT°						0.68	0.031 (0.87)	-0.200 (0.29)	0.133 (0.49)	-0.096 (0.62)	0.139 (0.47)
CORE							0.245 (0.20)	0.104 (0.59)	0.298 (0.11)	0.025 (0.89)	0.481 (0.008)

Table 2. Spearman's rank correlation ρ between network parameters (rows/first five columns) and between network parameters and mutational parameters (rows/last four columns). Abbreviations of network parameters are: BTW, betweenness centrality; CLO, closeness centrality; DEG, degree centrality; IN°, in-degree, OUT°, out-degree; CORE, core number. Network parameters are defined mathematically and heuristically in Table 1. Abbreviations of mutational parameters are: ΔM, per-generation change in the trait mean; |ΔM|, absolute value of ΔM; I_M, squared mutational coefficient of variation; I_E, squared residual coefficient of variation; h_M^2, mutational heritability. See text and Supplementary Table S1 for details of mutational parameters. Uncorrected P-values of mutational parameters are given in parentheses.

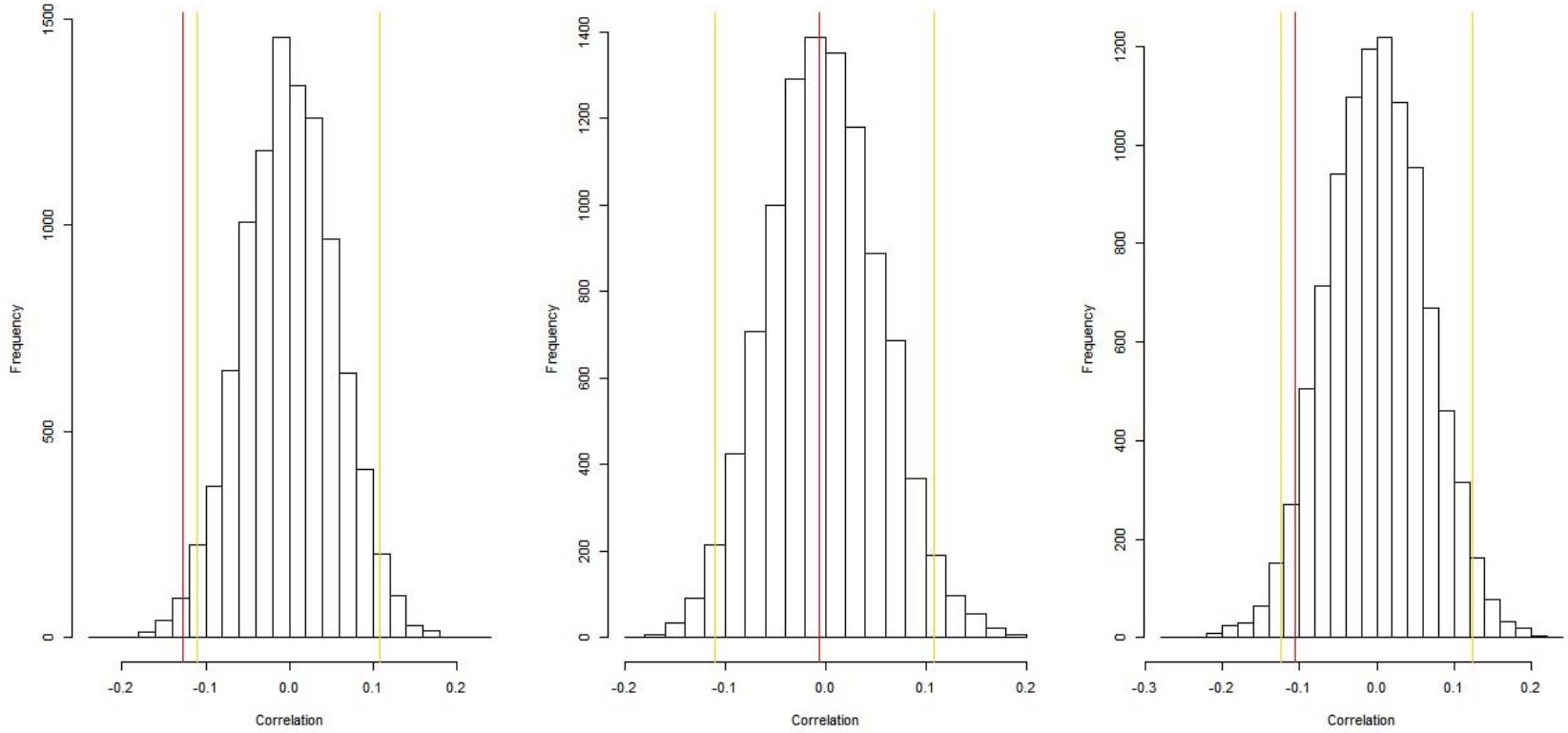

Supplementary Figure S1 - Parametric bootstrap distributions of random correlations ρ between (a) r_M and the shortest path length in the directed network, (b) $|r_M|$ and the shortest path length in the directed network, (c) r_M and shortest path length in the undirected network (i.e., the shorter of the two path lengths between metabolites *i* and *j* in the directed network). Red lines show the observed values of ρ, yellow lines show the 95% confidence interval of the distribution of the correlation between the mutational correlation and a random shortest path length drawn from the observed distribution of shortest path lengths. See Methods for details.

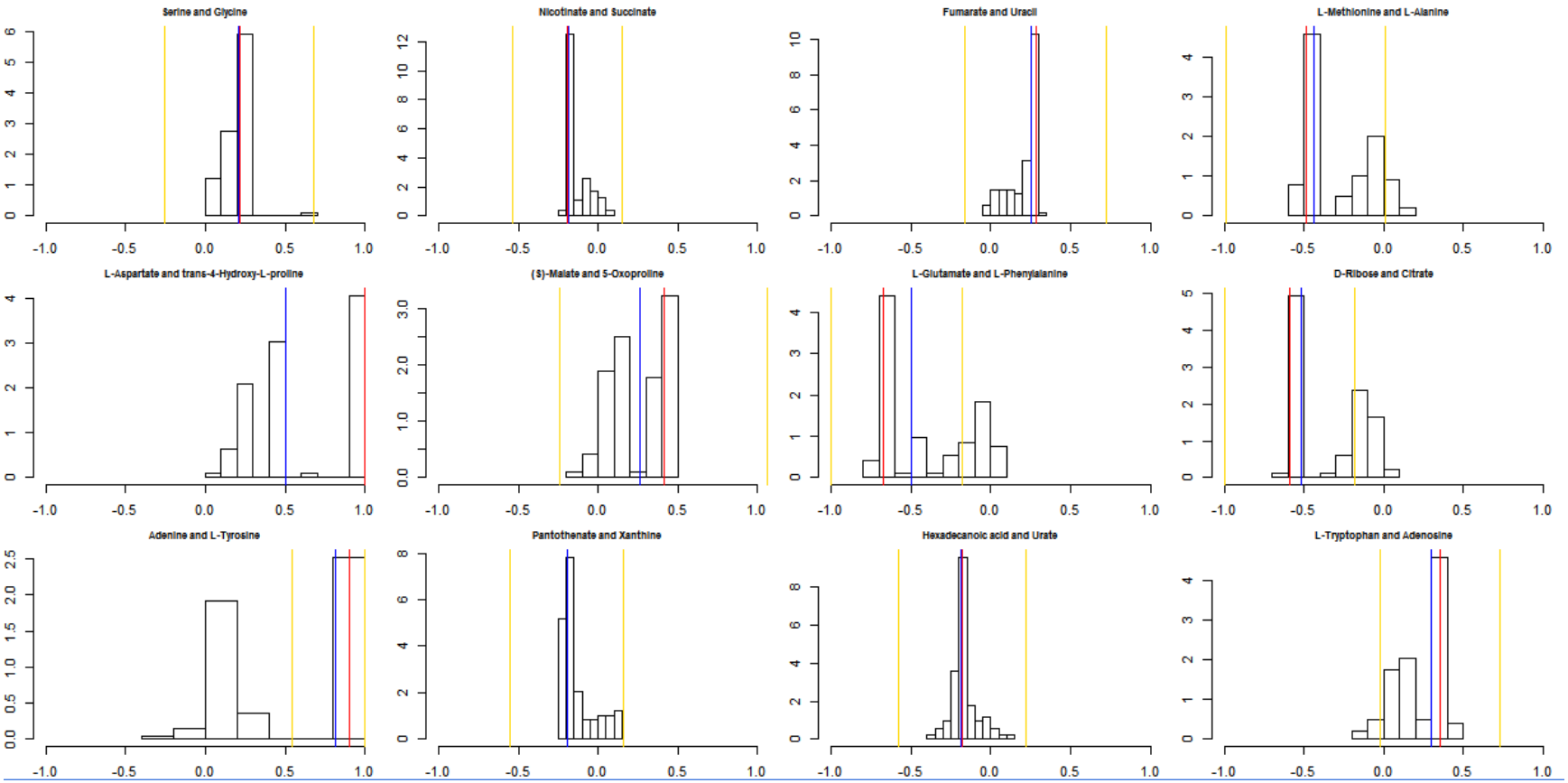

Supplementary Figure S2. Bootstrap distributions of mutational correlations (r_M) calculated from the joint REML estimate of the among-line components of covariance from a pair of focal metabolites (listed at the top of each panel) and six other metabolites randomly sampled without replacement. Each distribution is based on 100 resamples from the data. Red lines show the observed

r_M, blue lines show the median of the resampled values, yellow lines show $\pm$ two standard errors of the observed r_M. Details of the bootstrap analysis are given in the Methods.

Metabolite	***ID #***	**BTW**	**CLO**	**DEG**	**IN°**	**OUT°**	**CORE**
trans-4-Hydroxy-L-proline	11	0.004482	0.002761	0.004658	2	1	1
L-3-Amino-isobutanoate	10	0	0	0.001553	1	0	1
Adenine	20	0.003335	0.032205	0.009317	2	4	2
Adenosine	28	0.005516	0.032198	0.009317	4	2	2
L-Alanine	8	0	0	0.001553	1	0	1
L-Asparagine	16	0.002236	0.052579	0.004658	1	2	1
L-Aspartate	9	0.055054	0.056756	0.012422	3	5	2
Citrate	19	0.171567	0.058576	0.012422	4	4	2
Fumarate	6	0.028317	0.053784	0.007764	3	2	2
L-Glutamate	14	0.036659	0.048283	0.020186	5	8	2
Glycine	2	0.02661	0.044377	0.017081	5	6	2
L-Lysine	21	0	0.004658	0.004658	0	3	1
(S) – Malate	12	0.029016	0.057446	0.007764	2	3	2
L-Methionine	7	7.49E-05	0.004969	0.007764	2	3	2
Nicotinate	3	0.00221	0.046122	0.006211	2	2	2
Hexadecanoic acid	25	0.066162	0.019529	0.01087	2	5	2

Metabolite	*ID #*	BTW	CLO	DEG	In°	Out°	Core
Pantothenate	23	0	0.001553	0.001553	0	1	1
L-Phenylalanine	15	0.001137	0.040279	0.009317	1	5	1
Putrescine	18	0.003362	0.002795	0.003106	1	1	1
5-Oxoproline	13	0	0.045387	0.001553	0	1	1
D-Ribose	17	0	0.044346	0.001553	0	1	1
L-Serine	1	0.034582	0.057313	0.017081	5	6	2
Succinate	4	0.02215	0.051067	0.01087	4	3	2
Alpha,alpha-Trehalose	29	0	0.042179	0.001553	0	1	1
L-Tryptophan	27	0	0.004969	0.004658	0	3	1
L-Tyrosine	22	0.004518	0.041547	0.012422	3	5	2
Uracil	5	0.078303	0.044365	0.01087	4	3	2
Urate	26	0	0.029702	0.003106	1	1	1
Xanthine	24	0.004393	0.031003	0.01087	3	4	2

Supplementary Table S1(a), above. Network parameters for the 29 metabolites. Column headings are the abbreviations for the network parameters given in Tables 1 and 2. ID# is the number of the metabolite in the network shown in Figure 1.

Metabolite	***ID #***	***Mean (G0)***	***Mean (MA)***	***ΔM (%)***	***VL***	***VM***	***VE***	I_M	h_M^2 ***(x 10^3)***
trans-4-Hydroxy-L-proline	11	228.6 (10.4)	149.4 (14.5)	0.14 (0.02)	1058.0 (349.0)	2.12 (0.70)	3577.4 (1052.3)	9.45E-05	0.59 (0.26)
L-3-Amino-isobutanoate	10	20.0 (3.1)	14.5 (0.8)	-0.11 (0.06)	3.58 (4.32)	0.007 (0.009)	95.0 (9.86)	3.43E-05	0.08 (0.09)
Adenine	20	11.3 (1.4)	13.2 (0.8)	0.07 (0.06)	15.4 (4.4)	0.03 (0.009)	28.0 (4.02)	0.000178	1.10 (0.35)
Adenosine	28	2.1 (0.7)	26.0 (3.4)	4.39 (0.62)	407.7 (78.2)	0.82 (0.16)	186.5 (75.9)	0.001261	4.37 (1.97)
L-Alanine	8	5.5 (1.5)	6.1 (0.6)	0.04 (0.12)	5.48 (3.43)	0.011 (0.007)	30.3 (5.0)	0.000278	0.36 (0.23)
L-Asparagine	16	3.7 (1.3)	1.2 (0.1)	-0.27 (0.14)	0.11 (0.15)	0.0002 (0.0003)	2.4 (0.4)	0.000135	0.09 (0.13)
L-Aspartate	9	37.7 (2.7)	19.0 (1.2)	-0.20 (0.03)	48.2 (19.2)	0.096 (0.038)	60.2 (18.2)	0.00026	1.60 (0.80)
Citrate	19	11.4 (2.2)	5.7.1 (0.5)	-0.16 (0.08)	4.56 (1.54)	0.009 (0.003)	19.8 (6.8)	0.000182	0.46 (0.22)

Metabolite	***ID #***	***Mean (G0)***	***Mean (MA)***	***ΔM (%)***	***VL***	***VM***	***VE***	I_M	h_M^2 ***(x 10^3)***
Fumarate	6	33.0 (2.1)	25.5 (1.2)	-0.09 (0.03)	35.1 (9.2)	0.070 (0.018)	84.1 (26.1)	0.000109	0.83 (0.34)
L-Glutamate	14	115.2 (24.5)	93.2 (6.3)	-0.08 (0.09)	973.0 (556.8)	1.94 (1.11)	2703.7 (556.9)	0.000214	0.72 (0.44)
Glycine	2	47.1 (5.3)	52.8 (4.5)	0.05 (0.06)	606.7 (411.6)	1.21 (0.82)	939.3 (323.7)	0.000393	1.29 (0.98)
L-Lysine	21	6.7 (2.6)	5.0 (0.6)	-0.10 (0.16)	4.43 (3.99)	0.009 (0.008)	38.4 (7.01)	0.00032	0.23 (0.21)
(S) – Malate	12	44.7 (4.0)	71.9 (4.2)	0.24 (0.05)	397.8 (135.4)	0.80 (0.27)	1179.7 (276.2)	0.000157	0.67 (0.28)
L-Methionine	7	47.9 (4.1)	32.2 (1.7)	-0.13 (0.04)	101.2 (20.5)	0.202 (0.041)	72.4 (13.4)	0.000197	2.79 (0.77)
Nicotinate	3	4.9 (0.6)	33.0 (3.5)	2.29 (0.29)	473.9 (88.1)	0.95 (0.18)	120.3 (21.4)	0.000863	7.88 (2.03)
Hexadecanoic acid	25	238.4 (22.3)	265.1 (15.0)	-0.03 (0.04)	6712.9 (1579.6)	13.43 (3.16)	9579.1 (2985.7)	0.000194	1.40 (0.55)

Metabolite	***ID #***	***Mean (G0)***	***Mean (MA)***	***ΔM (%)***	***VL***	***VM***	***VE***	I_M	h_M^2 ***(x 10^3)***
Pantothenate	23	22.9 (0.8)	14.4 (0.6)	-0.15 (0.02)	12.8 3.2	0.026 (0.006)	16.0 (3.17)	0.000123	1.60 (0.51)
L-Phenylalanine	15	87.4 (7.9)	94.4 (6.3)	0.03 (0.05)	678.9 (263.6)	1.36 (0.53)	3835.0 (810.3)	0.000155	0.35 (0.16)
Putrescine	18	73.7 (15.3)	57.4 (3.4)	-0.09 (0.08)	70.9 (70.6)	0.14 (0.14)	1672.3 (193.2)	4.15E-05	0.08 (0.08)
5-Oxoproline	13	701.6 (40.0)	528.2 (22.2)	-0.10 (0.03)	7275.6 (3649.0)	14.56 (7.30)	52146.6 (13671.9)	5.24E-05	0.28 (0.16)
D-Ribose	17	5.6 (0.8)	13.3 (1.5)	0.51 (0.11)	76.3 (22.8)	0.15 (0.05)	66.3 (27.2)	0.000841	2.30 (1.17)
L-Serine	1	130.0 (49.8)	85.8 (3.7)	-0.14 (0.15)	373.7 (117.7)	0.75 (0.24)	1221.7 (376.9)	9.87E-05	0.61 (0.27)
Succinate	4	7.3 (0.8)	91.1 (9.7)	4.52 (0.51)	3216.6 (688.3)	6.43 (1.38)	2797.7 (932.6)	0.000778	2.30 (0.91)
Alpha,alpha-Trehalose	29	1772.2 (147.2)	2525.4 (277.6)	0.19 (0.07)	2118803 (105069)	4237.6 (2101.4)	4355039 (1656108)	0.000584	0.97 (0.61)

Metabolite	***ID #***	***Mean (G0)***	***Mean (MA)***	***ΔM (%)***	***VL***	***VM***	***VE***	I_M	h_M^2 ***(x 10^3)***
L-Tryptophan	27	107.7 (14.3)	92.2 (2.8)	-0.06 (0.05)	205.7 (87.3)	0.411 (0.174)	496.9 (64.0)	4.93E-05	0.83 (0.37)
L-Tyrosine	22	74.7 (9.3)	47.9 (2.9)	-0.14 (0.05)	197.2 (70.9)	0.394 (0.142)	643.3 (99.7)	0.00017	0.61 (0.24)
Uracil	5	9.5 (1.0)	8.8 (0.4)	-0.03 (0.05)	4.67 (1.59)	0.009 (0.003)	8.3 (1.4)	0.000123	1.13 (0.43)
Urate	26	20.7 (3.4)	11.5 (1.2)	-0.18 (0.07)	45.3 (20.1)	0.091 (0.040)	45.3 (4.75)	0.000654	2.00 (0.91)
Xanthine	24	0.4 (0.3)	6.7 (1.0)	6.64 (1.09)	36.5 (8.04)	0.073 (0.016)	15.5 (2.8)	0.001711	4.70 (1.34)
Mean			0.73* (0.30)				1.46 (0.31)		
Median			0.14				0.83		

Supplementary Table S1(b). Mutational statistics of the 29 metabolites, reprised from Supplementary Table S1 of Davies et al. (2016). Column Headings are: *ID#*, the number of the metabolite in the network shown in Figure 1; *Mean (G0)*, mean metabolite pool of the G0 ancestor; *Mean (MA)*, mean metabolite pool of the MA lines; *ΔM (%)*, percent change per-generation in mean trait

value; *VL*, among-line component of variance, *VM*, mutational variance; $CV_{M,G0}$, mutational coefficient of variation standardized by the G0 mean; $CV_{M,MA}$, mutational coefficient of variation standardized by the MA mean; *VE*, environmental (= within-line) component of variance; h_M^2, mutational heritability.

* - Mean *ΔM (%)* is the mean absolute value.

Reaction Number	Reaction
R01579	D-Glutamine + H2O = D-Glutamate + NH3
R01887	gamma-Amino-gamma-cyanobutanoate + 2 H2O = DL-Glutamate + NH3
R04936	Se-Adenosylselenohomocysteine + H2O = Adenosine +Selenohomocysteine
R00891	L-Serine + Hydrogen sulfide = L-Cysteine + H2O
R09099	L-Serine + 5,6,7,8-Tetrahydromethanopterin = 5,10-Methylenetetrahydromethanopterin + Glycine + H2O
R02853	D-O-Phosphoserine + H2O = D-Serine + Orthophosphate
R00904	3-Aminopropanal + NAD+ + H2O = beta-Alanine + NADH + H+
R03542	alpha-Aminopropiononitrile + 2 H2O = Alanine + NH3
R01324	Citrate = Isocitrate
R00483	ATP + L-Aspartate + NH3 = AMP + Diphosphate + L-Asparagine
R01221	Glycine + Tetrahydrofolate + NAD+ = 5,10-Methylenetetrahydrofolate+ NH3 + CO2 + NADH + H+
R02078	3,4-Dihydroxy-L-phenylalanine + L-Tyrosine + Oxygen = Dopaquinone+ 3,4-Dihydroxy-L-phenylalanine + H2O
R01706	Hexadecanoyl-[acp] + H2O = Acyl-carrier protein + Hexadecanoicacid
R04666	3-Ureidoisobutyrate + H2O = 3-Aminoisobutyric acid + CO2 + NH3

Supplementary Table S2. Discrepancies between the metabolic networks constructed using the MZ and YW methods. All reactions listed here are in the Ma and Zeng database (http://www.ibiodesign.net/kneva/) but not in the Wormflux database (http://wormflux.umassmed.edu/) and were used in the generation of the metabolic network. There is a total of 1203 reactions in the network, these represent about 1% of all reactions.